Title
The crystallographic structure of brome mosaic virus11Edited by I. A. Wilson

Journal
Journal of Molecular Biology, 317(1)

ISSN
0022-2836

Authors
Lucas, Robert W
Larson, Steven B
McPherson, Alexander

Publication Date
2002-03-01

DOI
10.1006/jmbi.2001.5389

doi:10.1006/jmbi.2001.5389 available online at http://www.idealibrary.com on IDEAL® J. Mol. Biol. (2002) 317, 95–108

JMB

The Crystallographic Structure of Brome Mosaic Virus

Robert W. Lucas, Steven B. Larson and Alexander McPherson*

University of California, Irvine
560 Steinhaus Hall, Irvine
CA 92697-3900, USA

The structure of brome mosaic virus (BMV), the type member of the bromoviridae family, has been determined from a single rhombohedral crystal by X-ray diffraction, and refined to an *R* value of 0.237 for data in the range 3.4-40.0 Å. The structure, which represents the native, compact form at pH 5.2 in the presence of 0.1 M Mg^{2+}, was solved by molecular replacement using the model of cowpea chlorotic mottle virus (CCMV), which BMV closely resembles. The BMV model contains amino acid residues 41-189 for the pentameric capsid A subunits, and residues 25-189 and 1-189 for the B and C subunits, respectively, which compose the hexameric capsomeres. In the model there are two Mg ions and one molecule of polyethylene glycol (PEG). The first 25 amino acid residues of the C subunit are modeled as polyalanine. The coat protein has the canonical ''jellyroll'' β-barrel topology with extended amino-terminal polypeptides as seen in other icosahedral plant viruses. Mass spectrometry shows that in native BMV virions, a significant fraction of the amino-terminal peptides are apparently cleaved. No recognizable nucleic acid residue is visible in the electron density maps except at low resolution where it appears to exhibit a layered arrangement in the virion interior. It is juxtaposed closely with the interior surface of the capsid but does not interpenetrate. The protein subunits forming hexameric capsomeres, and particularly dimers, appear to interact extensively, but the subunits otherwise contact one another sparsely about the 5-fold and quasi 3-fold axes. Thus, the virion appears to be an assembly of loosely associated hexameric capsomeres, which may be the basis for the swelling and dissociation that occurs at neutral pH and elevated salt concentration. A Mg ion is observed to lie exactly on the quasi-3-fold axis and is closely coordinated by side-chains of three quasi-symmetry-related residues glutamates 84, with possible participation of side-chains from threonines 145, and asparagines 148. A presumptive Mg^{2+} is also present on the 5-fold axis where there is a concentration of negatively charged side-chains, but the precise coordination is unclear. In both cases these cations appear to be essential for maintenance of virion stability. Density that is contiguous with the viral interior is present on the 3-fold axis at the center of the hexameric capsomere, where there is a pore of about 6 Å diameter. The density cannot be attributed to cations and it was modeled as a PEG molecule.

*Corresponding author

Keywords: assembly; stability; metalions; dissociation; diffraction

Introduction

Brome mosaic virus (BMV), a $T = 3$ icosahedral virus, is the type member of the bromoviridae family and bromovirus genus.[1] It infects many species of gramineae and can be easily transmitted mechanically, as well as by various vectors.[2] It is composed of 180 identical polypeptides which assume an equal number of either an A, B, or C conformation, and a multipartite genome consisting of four single-stranded RNA molecules of 3.2 kb, 2.8 kb, 2.1 kb and 0.8 kb designated RNA1, RNA2, RNA3, and RNA4, respectively. RNA1 and RNA2 are found alone in virions, while RNA3 and RNA4, the latter of which codes only for the coat protein,[3] are found packaged together. Thus, the

Abbreviations used: BMV, brome mosaic virus; PEG, polyethylene glycol; CCMV, cowpea chlorotic mottle virus.

E-mail address of the corresponding author: amcphers@uci.edu

0022-2836/02/010095–14 $35.00/0

total complement of RNA in any of the three types of particles is roughly the same. The coat protein is composed of 189 amino acid residues, with a highly positively charged amino-terminal segment.

BMV is one of the most thoroughly investigated of all of the spherical plant viruses, and it is neither possible nor necessary to review all of the information available on its structure, assembly, or physico-chemical properties.[2,4–6] A number of points are, however, directly pertinent to this investigation and its results. BMV is similar in most regards to the closely related cowpea chlorotic mottle virus (CCMV) whose structure has been determined elsewhere [7]. It has a diameter of about 28 nm in the native state at low pH (< 6.0) and in the presence of Mg^{2+}, but experiences a profound, though reversible, structural transition as the pH approaches neutrality.[8–10] Mg^{2+} helps stabilize the native virion at higher pH, but does not prevent the transition.[11,12] The transition may be regulated by carboxyl clusters and be mediated by cations as proposed for other virions as well.[13] At high salt conditions and neutral pH, the virion loses its RNA and dissociates into protein products. The protein can be reassembled under defined conditions into a variety of forms, including both empty $T = 3$ and $T = 1$ icosahedra.[14–18]

Most physico-chemical evidence suggests that there are only weak interactions in the capsid between individual protein subunits, though the data equally support weak interactions between capsomeric groups of subunits. Hence, empty icosahedral shells are not observed *in vivo* and assembly, unlike that for tymoviruses, is apparently not driven by protein-protein interactions and capsid formation. Instead, assembly seems to proceed by concerted interactions between the very positively charged amino-terminal polypeptides of the coat proteins and more or less globular, preformed masses of negatively charged RNA. Thus, the virions are believed to be created and maintained principally by relatively fluid protein-nucleic acid interactions.[4]

Nearly 60 years of experimentation on BMV indicates that the virus is among the least rigid in terms of structure, most malleable in terms of form, and most susceptible to transitions. Intersubunit interactions appear weak and imprecise; protein-RNA interactions are non-specific, and encapsidation criteria meager.[11,19] The structure we present here suggests explanations for a number of these features, and also suggests a mechanism for assembly and disassembly compatible with the observations.

Results

The asymmetric unit in the *R*3 crystals[8] is composed of 20 triangular faces each containing three icosahedrally distinct protein subunits designated A, B and C. All have identical amino acid sequences but assume three different subunit conformations to accommodate their structural roles in the virion. Therefore, 20-fold non-crystallographic symmetry was used in all averaging operations and maintained throughout refinement. In the model of BMV, the pentameric A subunits were composed of residues 41-189, the B and C subunits comprising the hexameric capsomeres of residues 25-189 and 1-189, respectively. Amino-terminal segments of the A and B subunits were not visible in electron density maps. The initial 25 amino acid residues at the amino-terminal ends of the C subunits were observed as continuous chains, contiguous with the remainder of the C subunits at amino acid 26, but they were somewhat disordered. These C subunit amino-terminal peptides were, therefore, modeled as polyalanine chains.

The protein subunits are shown as they are assembled to make pentameric capsomeres (from A subunits), hexameric capsomeres (from B and C subunits), and distributed about the quasi-3-fold axis (A, B, and C subunits) in Figures 1, 2 and 3, respectively. The coat protein exhibits the canonical ''jelly roll'' β-barrel topology with amino-terminal polypeptides ultimately extended into the interior of the virus. The visible portions of the amino-terminal polypeptides of the B and C subunits form a distinctive ''β annulus'' about the 3-fold axis at the center of each hexameric capsomere, as seen in a number of other icosahedral viruses.[20] The hexamer is characterized by a pore at its center of about 6 Å diameter and the pentamer by a similar channel of about 5 Å diameter.

The pore through the hexameric unit is obstructed. This is illustrated by density, shown in Figure 4, that appears to be contiguous with disordered density in the interior. It could conceivably be nucleic acid, or amino-terminal polypeptides from either intact coat proteins or fragments from cleaved subunits, but these do not appear likely. It may also be ordered water, PEG, or disordered ions, but does not appear to be discreet cations such as Mg^{2+} or Ca^{2+}. The amino acid side-chains making closest approach to the density are two valine residues, 30 and 32, from the B and C subunits. There are no charged residues in the channel and it appears to be hydrophobic in character. We have modeled this density with what we feel is the most innocuous choice, a PEG molecule.

In addition to the three protein subunits, Mg ions were included on the quasi-3-fold axis and the 5-fold axis, based on pronounced spherical peaks at those positions in the electron density maps (3 σ in $2F_o - F_c$ composite omit maps). The Mg^{2+} on the 5-fold axis is at a radius of 127 Å from the center of the virus particle. Although there are a number of negatively charged amino acid side-chains in the immediate area, which are directly involved is uncertain and the binding of the ion may be mediated through water molecules. No water molecules were included, however, because of the modest resolution of the data. The ion, in any case, effectively blocks this channel.

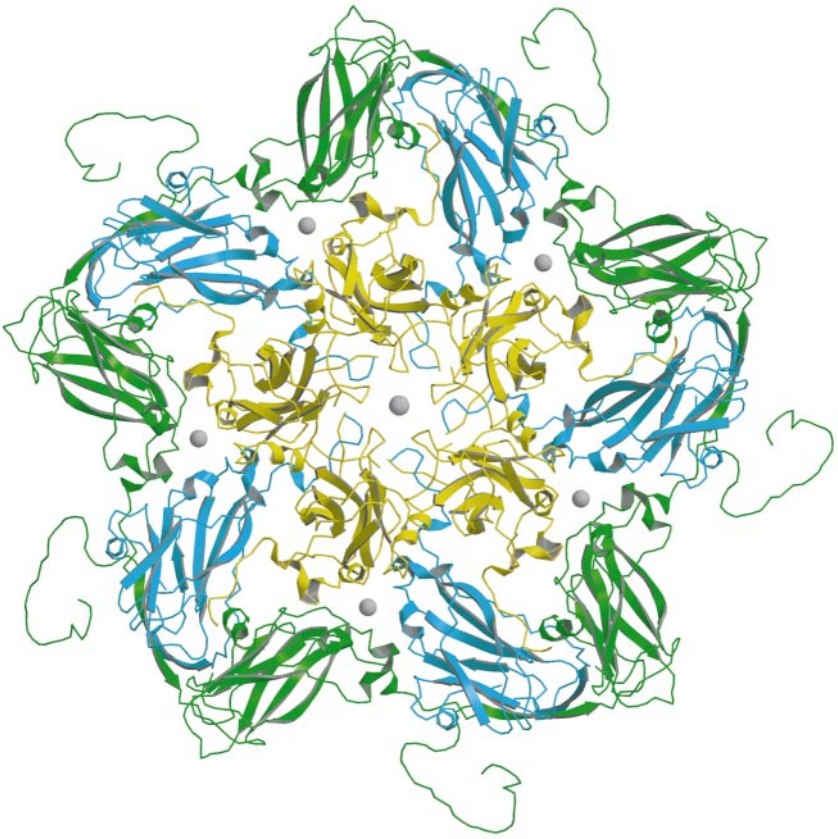

Figure 1. The pentameric A subunits are shown here as yellow ribbons along with a central cation bound by backbone carboxylate groups. The B and C subunits are cyan and green, respectively; the cations on the quasi-3-fold axes are also present.

Precisely on the quasi-3-fold axis is a Mg ion coordinated directly by three carboxyl groups provided by quasi-symmetric glutamates 84 from the A, B and C subunits, as illustrated in Figure 5. The three carboxyl groups of glutamates 84 are within 2.6 Å of the Mg^{2+}. Within 5 Å to 6 Å of the Mg^{2+}

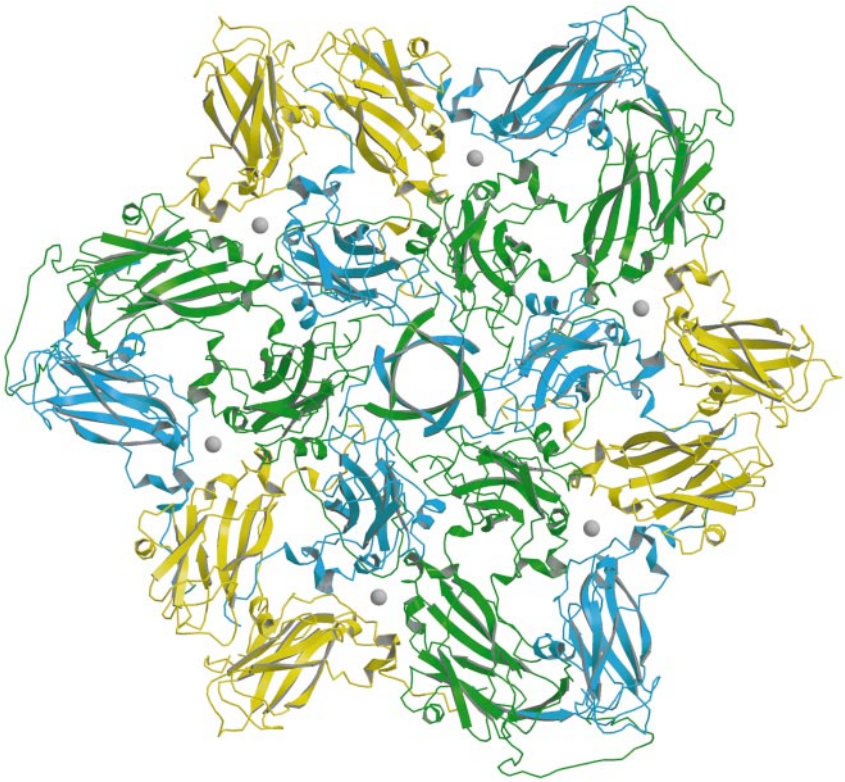

Figure 2. The B and C hexameric subunits are shown in cyan and green, respectively, and 5-fold A subunits, with which they make contacts, are yellow. The β-annulus at the center of the capsomere forms a pore of about 6 Å diameter. Ions on the quasi-3-fold axes are also shown.

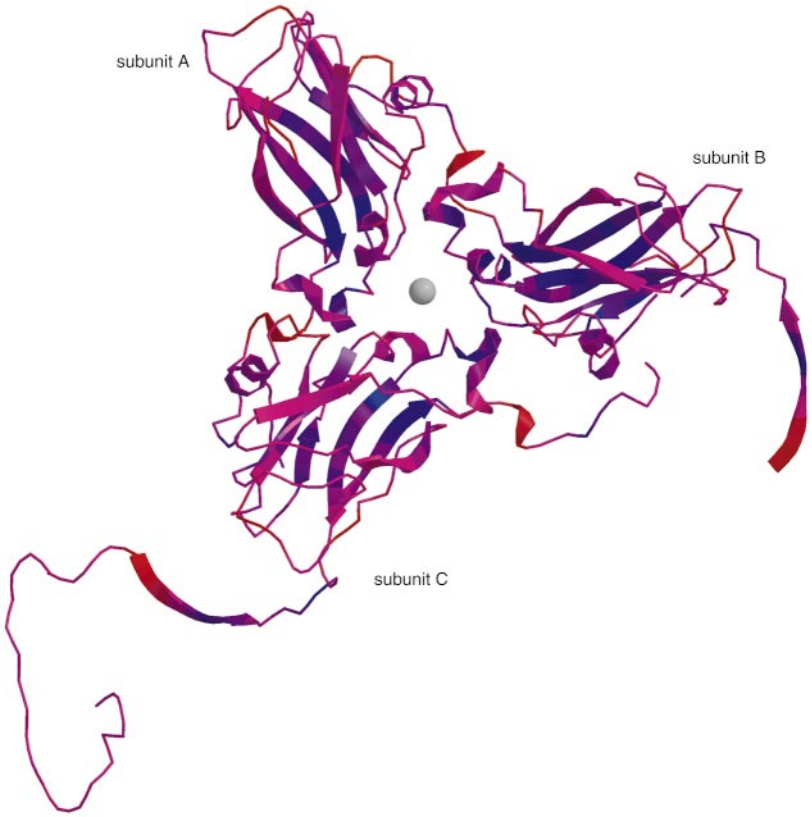

Figure 3. A ribbon diagram of the BMV A, B and C subunits colored according to thermal factor *B*. Red indicates areas of higher value while blue indicates less mobile regions.

are the three side-chain oxygen atoms of threonines 145, and the three side-chain carboxyl groups of quasi-equivalent aspartic acids 148. All of these could be bridged to the cation through water molecules. Thus, within a sphere of radius 6 Å about the Mg^{2+}, there are six negatively charged carboxyl

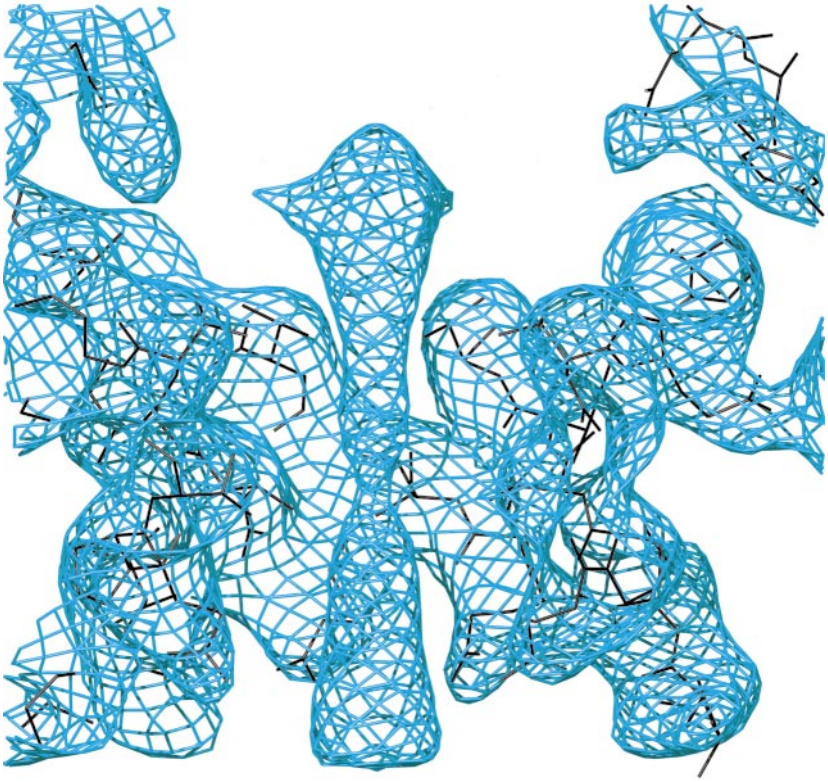

Figure 4. The channel through the center of the hexameric capsomere is filled with density in this $2F_o - F_c$ map that cannot be readily explained by either protein or nucleic acid. It has been modeled as a 3-fold disordered molecule of polyethylene glycol and probably originated from the crystallization mother liquor.

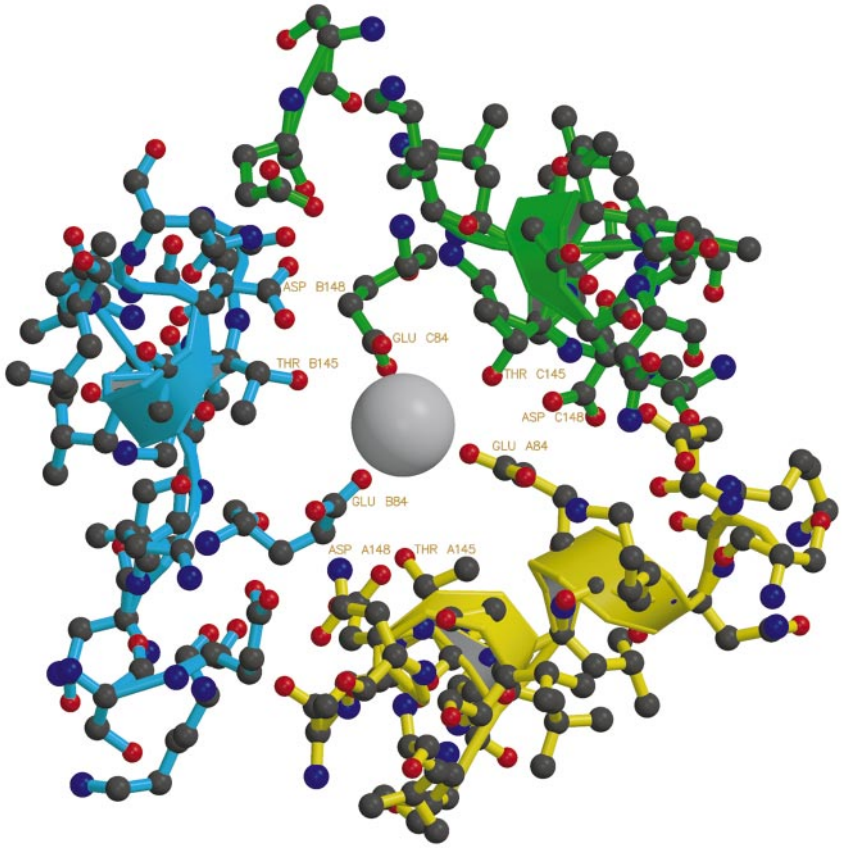

Figure 5. The coordination of the Mg ion on the quasi-3-fold axis. The glutamate, threonine, and aspartate residues involved are labeled. These cations may serve a crucial role in the formation and maintenance of the capsid structure, and the carboxyl groups are likely those earlier identified as Caspar carboxyls.[13]

groups plus three additional oxygen atoms. This Mg ion appears to play a particularly important role in maintaining the structure of the capsid and is likely the source of the cation stabilization of the native virion. Were it removed, then only water would remain to mediate the close carboxyl interactions. Such an arrangement involving Mg^{2+} was suggested by Speir *et al.*[7] for CCMV as well.

The weakest interactions are amongst ABC subunits at the quasi-3-fold axes, and amongst A subunits about the 5-fold axes. This is evident in Figure 6. The occluded surface areas at these interfaces are only about half those for the dimer interfaces and those within the hexameric capsomeres. Inspection of the dimer and hexamer interface areas, which are about 1000 $Å^2$ or greater, shows that these are due almost entirely to contacts involving the amino and carboxy-terminal polypeptides. Removal of residues 1-49 and 177-189 at the two termini virtually eliminates any contact. The extensive contact areas characterizing the dimers, which range from 1244 to 1589 $Å^2$, suggest that the dimers may be the molecular species responsible for assembly.

Moderate subunit interactions woven together *via* interdigitating carboxy termini may help to explain the capsid plasticity characteristic of bromoviruses. These may facilitate the observed capsid swelling preceding irreversible disruption of the virus shell.[7,21] The presence of stabilizing Mg ions, which serve as lynchpins at 5-fold and quasi-3-fold axes, would explain how cations stabilize the capsid above neutral pH. In the absence of these ions, increased pH would promote repulsive interactions, thereby causing the capsid to dissociate. The ultimate products are presumably AB and CC dimers held together by the interwoven carboxy termini.[18,22]

The appearance of the intact virion is seen in Figure 7 along with relevant dimensions. The plane cutting through the capsid in Figure 7 contains both the 5-fold and 3-fold axes. It presents the electrostatic distribution across the viral shell, and through the channels at the two axes. At the top of Figure 7 the exterior and interior electrostatic surfaces of the protein capsid are shown. As one might expect, the interior surface of BMV, even in the absence of the basic amino-terminal polypeptides, is very positively charged and undoubtedly closely associated with negatively charged RNA.

Proteolytic cleavage of N-terminal polypeptides

We found in a separate study[8] that dissociation of the virions to produce capsid protein, and protein assemblies, was accompanied by proteolytic cleavage of amino-terminal polypeptides from a portion, and sometimes all of the protein subunits. Mass spectrometry of BMV from rhombohedral

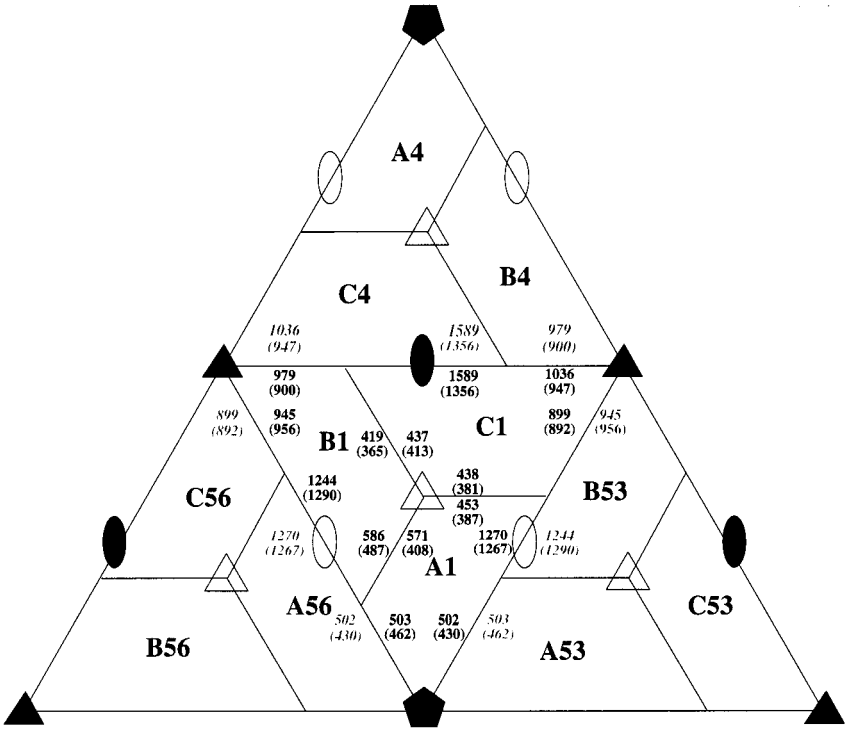

Figure 6. A diagram of the BMV capsid showing contacting surface areas for the symmetry-related protein subunits. Along each unique interface the surface area buried by that interface is noted. The values in parentheses are those for the closely related CCMV structure. This provides some measure of the degree of interaction of two subunits across each interface. Exact rotation axes are identified by filled symbols and quasi rotation axes by open symbols.

crystals used in this X-ray diffraction analysis shows some degree of cleavage in these capsid subunits as well. Intact subunits comprise the majority of the population, but some subunits are cleaved to produce significant subpopulations of subunits $M_r = 14{,}533$ and $M_r = 10{,}180$, corresponding to N-terminal cleavages at amino acid residues 57 and 97, respectively. In addition, mass spectrometry also shows at least three peptides, presumably cleavage products, also present in the crystals, and almost certainly in the virions. These have molecular masses of about 5808 Da, 4770 Da, and 4430 Da and are likely to be the complements, or additionally degraded complements of the subunits.

We cannot be certain whether the visibility and more ordered conformation of the amino-terminal polypeptides of the C subunits have functional significance or not. The C subunits may simply be less susceptible to proteolytic cleavage, or their amino termini may make more defined contacts with the RNA. On the other hand, amino-terminal polypeptides of the C subunits may be more visible and ordered because they play some special role in guiding the arrangement of the capsid protein about the RNA cores, and in promoting assembly.

Comparison to CCMV

The sequences of BMV and CCMV are 70% identical and highly homologous over the remainder. The sequence of BMV is one amino acid residue shorter than that of CCMV due to deletions at 27 and 150 in the CCMV sequence, and the addition of an arginine residue at the carboxy terminus. The deletions occur at the start of the β-annulus and at the end of the GH helix.[7] Both changes are accommodated easily. Most other differences between the structures appear in loops connecting β-strands of sheets. Both BMV and CCMV have highly positively charged amino-terminal polypeptides that contain one arginine and seven lysine residues for BMV, and three lysine and six arginine residues for CCMV. Given the degree of homology, it is not surprising that the structures of the coat proteins of the two viruses are nearly the same. The differences in amino acids between the two, as seen in Figure 6, accumulate at subunit interfaces in the capsid, and therefore result in significant differences in intersubunit contacts.

The A, B and C subunits of BMV exhibit rms differences for C^{α} positions of 0.88 Å (A-B), 1.01 Å (A-C), and 0.99 Å (B-C). The superposition of corresponding subunit backbones of BMV on the CCMV model is shown in Figure 8. The correlations between equivalent C^{α} positions for BMV and CCMV subunits are equally good with 1.02 Å, 1.08 Å and 1.06 Å RMS differences for the A, B and C subunits, respectively. The most striking differences between the two structures arise as a consequence of the bound cations. CCMV was crystallized for X-ray diffraction at pH 3.3 in the presence of EDTA and contained no cations. The rhombohedral BMV crystals studied here were purified and crystallized in the presence of 0.1 M magnesium acetate at pH 5.2. As a consequence, cations were observed in the structure.

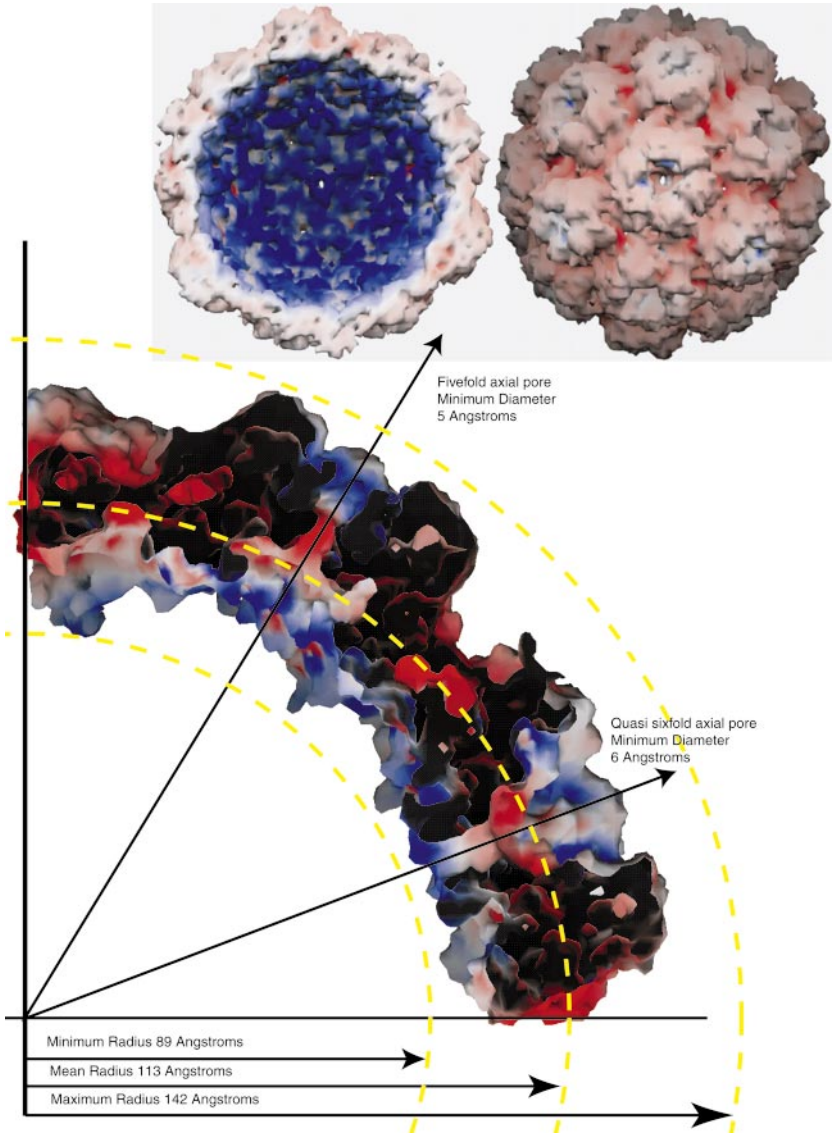

Figure 7. A quarter cross-section through the BMV capsid. The plane of the cross-section includes the 5-fold and 3-fold axes that pass through the centers of the pentameric and hexameric capsomeres. The surfaces are colored according to their electrostatic character; red is negative, blue positive, and gray neutral. Inset at the top contains electrostatic surfaces of the exterior of the BMV capsid on the right and on the left an interior electrostatic surface. Both images were created using the program GRASP.[42]

RNA distribution

The distribution of difference density in the $F_o - F_c$ map of BMV is not entirely arbitrary inside the virion, though there are no elements of density that can be interpreted unambiguously as either single or double-stranded RNA. The observed density appears simply to be where fortuitous superpositions of RNA density occurred during the averaging processes (both physical during crystallization, and computationally during map averaging). The difference density is, however, organized into two shells.

In agreement with low angle neutron scattering studies,[23–25] there is a lumen at the center of the particle of about 35 Å radius. This is presumably occupied by bulk solvent. From about 35 to 65 Å radius, there is a shell occupied by substantial density, then a distinctive trough until a radius of about 75 Å. Between that radius and the inside of the protein capsid is the strongest band of density. This density does not appear to extend into the protein shell to any appreciable degree except at the centers of the hexameric capsomeres (the 3-fold axes) where density (modeled as a PEG molecule) is seen in the pore. The pore, however, is only 6 Å in diameter so it is difficult to envision how this could represent main-chain RNA. Indeed, there appears to be close apposition of RNA to the interior of the protein shell, consistent with the observed positive electrostatic surface on the inside of the capsid, but there is no visible penetration.

Because the distribution of the RNA is not uniform in the capsid, estimates of the RNA packing density may have to be re-evaluated. Assuming a more or less uniform RNA distribution between radii 30 and the inside of the capsid, Anderegg *et al.*[25] calculated that this region was composed of about 50 % solvent and that, therefore, the RNA was rather loosely assembled. If, however, it exists

Figure 8. Backbone representation superimposing the BMV ABC trimer on the corresponding CCMV trimer, which is presented as a transparent overlay.

predominantly in two shells with a solvent volume interposed, then the packing of the RNA in the two shells would be significantly greater than the overall average. A greater local packing density might be more consistent with the nearly 60% base-paired secondary structure of the RNA predicted from circular dichroism.[5]

Discussion

Subunit interactions and structural transitions

Most studies of the physical structure of BMV have suggested that only tenuous interactions exist between protein subunits in the capsid, and that virion integrity is maintained principally by protein-RNA interactions (for a discussion, see Kaper[4]). An examination of the structure shows the situation to be somewhat more complicated. Within hexameric capsomeres, but to a considerably lesser extent pentameric capsomeres, subunit interfaces are relatively large and the interactions extensive, comparable to those in other $T = 3$ viruses. The interactions between capsomeres, i.e. those around the quasi-3-fold axis where A, B, and C subunits join, are meager. In addition, a principal component of the assembly at the quasi-3-fold, perhaps the lynchpin of the capsid structure, is the Mg ion that is coordinated by negatively charged side-chains from each of the three subunits.

Indeed, were the Mg^{2+}, which is known to stabilize the structure and modulate swelling[11] removed, then the charged carboxyl groups from glutamates 84 and aspartates 148 would repel one another. This would not only further weaken the bonding at the quasi-3-fold, but would introduce a destabilizing influence. These carboxyl groups, in the absence of Mg^{2+}, as in CCMV, may be the crucial carboxyl clusters suggested to control the swelling of BMV and its ultimate disassembly.[11,12]

The susceptibility of the structure at the quasi-3-fold axes coupled with firmer interactions within capsomeres suggests that upon dissociation of the capsid, the immediate products would be RNA, and probably protein hexamers (B and C subunits) and dimers. This is consistent with what is observed by AFM in the transition of $T = 3$ to $T = 1$ particles.[8] On the other hand, there is evidence that dissociated capsids ultimately yield dimers in solution.[18,22] This is realistic as well because protein-protein interactions across icosahedral dyad axes are also extensive (see Figure 6, above).

RNA distribution

Evidence acquired over the past 40 years of research on BMV and CCMV consistently suggests that the structure of the virion is maintained principally by protein-RNA interactions with otherwise weak intersubunit contacts. The close approach of the RNA to the inside of the protein shell, and the positively charged interior surface is consistent with this view. Likely to be at least as important, however, are the highly positively charged amino-terminal polypeptides. These have clearly been shown essential to virion assembly,[26,27] protein-RNA interactions,[11] virion integrity,[4] swelling stages of the virion,[9,10] and a number of other

structural and physiological properties.[5] These are ambiguous or not observed at all in the electron density map and are probably associated with the outer shell of RNA. They may serve as anchors and lines to moor the individual protein subunits to the RNA core. Thus, the protein units on the surface may experience only tenuous lateral interactions among themselves while tethered to the core. Such an imprecise capsid arrangement could explain the relatively poor diffraction properties of the various crystals of this virus, and why crystals of the BMV $T = 1$ particles lacking RNA, but requiring much closer protein-protein contacts, diffract to substantially higher resolution.[8]

Protein-nucleic acid interactions and assembly

Icosahedral averaging, both physical upon crystallization and computational in map averaging, suppresses nucleic acid density inconsistent with viral symmetry. Frequently, however, bits and pieces, and occasionally large segments of nucleic acid are visible in electron density maps of spherical viruses where the RNA or DNA does, through virion design, appear systematically consistent with the icosahedral symmetry (see Larson & McPherson for examples).[28] No discrete elements of nucleic acid, however, were apparent in this BMV structure.

This is, perhaps, not surprising. The BMV coat protein encapsidates RNA1, RNA2, or RNA3 plus RNA4. The RNAs are completely dissimilar in sequence, and RNA3 + RNA4 consists of two independent entities. They would be unlikely to share the same secondary and tertiary structures, form similar cores, or be capable of systematically making the same specific interactions. The only common features they are likely to exhibit are a final core size and a display of negatively charged phosphate ions. It is not unexpected, then, that the principal protein-nucleic acid interactions would be electrostatic and non-specific in nature. This is consistent with the very positively charged inner surface of the BMV capsid, and the positively charged, and structurally critical, amino-terminal polypeptides.

There are three plausible mechanisms for the assembly of small icosahedral viruses. Either (1) encapsidation proceeds through highly cooperative interactions between the RNA and protein in which the nucleic acid assumes its virion conformation as a consequence of its interactions with proteins. This was proposed for satellite tobacco mosaic virus (STMV).[28] Another means (2) is where the RNA folds independently into some roughly spherical core structure, purely as a consequence of secondary and tertiary nucleic acid interactions, and the protein shell then forms around it by virtue of non-specific charge interactions involving positively charged subunits and negatively charged phosphate groups. A third possibility (3) which might be operable, and is likely in the case of the tymoviruses,[4] is that a nearly complete capsid forms entirely through protein-protein interactions, and the RNA is then drawn into the capsid, again, probably through charge interactions.

In (1) there must be strong protein-nucleic acid interactions, some consistent with icosahedral symmetry and, therefore, occasionally visible in electron density maps.[20,28] No such interactions are seen in BMV. Mechanism (3) is characterized by rigorous protein-protein interactions and the *in vivo* formation of empty capsids. All physico-chemical evidence suggests this not to be the case for BMV. Indeed, *in vivo*, bromoviruses apparently form no empty capsids.[22] The structure of BMV suggests that mechanism (2) is more likely responsible for assembly.

The fact that BMV can encapsidate RNA1, RNA2, or RNA3 + RNA4, which share no sequence homology, and, therefore, probably no secondary and tertiary motifs, weigh against specific interactions. Yet, protein-nucleic acid interactions have been shown to be crucial in virion assembly and maintenance.[4,11] Other evidence[26,27] indicates that interactions between protein and RNA are essential for proper assembly, and are mediated principally through the amino-terminal polypeptides, which we observe to be spatially disordered for A and B subunits, and partially for the C subunits as well.

The model that emerges, then, is that the RNAs likely fold into globular forms that present negatively charged binding sites for the amino-terminal tails. By these tails, protein subunits are drawn together and loosely organized around the RNA where protein-protein interactions ultimately direct formation of the icosahedral capsid. The amino-terminal tails subsequently remain as electrostatic anchors in the RNA cores to effect virion cohesion. Swelling and disassembly occurs when those anchors are disrupted or cleaved from the protein units, or their tethers to the protein subunits are weakened by extension.

An additional observation that supports mechanism (2) is that reassembly of BMV protein around its various RNAs to produce intact virions is virtually instantaneous.[29] Were significant rearrangement of RNA structure required, or a series of protein aggregation steps necessary to form partial capsids, then the speed of the reassembly reaction would not likely be so great. The reaction suggests rapid initiation and propagation accompanied by cooperative structural interactions.

The swelling process

One of the most thoroughly studied aspects of the behavior of BMV is the swelling transition the virion experiences between pH 6 and 7. This transition is particularly pronounced in the absence of Ca^{2+} or Mg^{2+}, which otherwise stabilize the virion. The structure presented here is consistent with a number of earlier proposals regarding that tran-

sition. First, carboxyl groups are involved. These are seen at the quasi-3-fold axes and 5-fold axes where they interact with Mg ions and, thereby, also explain the cation stabilization. Removal of those cations would allow mutual repulsion of the carboxyl groups and promote subunit separation, and perhaps disassembly. Weak protein-protein interactions between subunits were also predicted[4], and they were observed here between capsomeres, also consistent with the transition. Finally, the disorder of the positively charged amino-terminal tails of the coat proteins is consistent with a loose and rather non-specific interaction with the RNA, seemingly another requirement for the transition. We see no evidence, however, that cations regulating the transition bind directly to the encapsidated RNA as has been suggested.[12]

RNA4 and the evolution of satellite viruses

A possible mechanism for the origin of $T = 1$ satellite viruses, such as STMV, satellite tobacco necrosis virus (STNV) and satellite panicum mosaic virus (SPMV), is that they evolved from a recombination product in host cells which were multiply infected with larger viruses.[30] The replicase recognition site of the helper virus, which must be a common feature, defined the helper virus specificity, and, therefore, also conferred the host range. The coat protein, however, very probably came from elsewhere, i.e. another virus.

We raise this issue because of the several RNAs found in BMV and other multipartite $T = 3$ icosahedral viruses. Certain correlations can be made, particularly regarding the curious RNA4 species. RNA4 in BMV is about 800 nucleotides in length and has about 65% internal base-pairing capability.[6,31,32] This is approximately the same as for the satellite virus RNAs (SPMV/820 bases, STMV/1058 bases, STNV/1260 bases). RNA4 has a replicase recognition site, as do satellite virus RNAs. RNA4 codes only for the viral coat protein, and this is the only function presently assigned to the satellite virus RNAs. Finally, when truncated or incomplete RNAs are encapsidated, the product is frequently a $T = 1$ virus having the properties of the satellite viruses.[8,16]

While these observations are only suggestive, it is not unreasonable to speculate that the satellite virus RNAs may have been derived from RNA4 species of multipartite viruses. Of course the converse might also be considered, but because of the involvement of RNA3, this would necessarily be a more intricate and less probable process.

Materials and Methods

Growth and purification of BMV

BMV was obtained from Dr A. L. N. Rao at the University of California Riverside and propagated in barley plants (*Hordeum vulgare* cv. Dickson) in a greenhouse. At the one leaf stage (approximately one week after sprouting) plants were abrasively scarred with diatomaceous earth and BMV virus solution was then applied to the wound site. Infected plants exhibited narrow, subtle, longitudinal striations along their leaves and were harvested and frozen at −70 °C prior to virus purification.

Frozen BMV leaves were mixed in a blender with two parts of extraction buffer (0.5 M sodium acetate, 80 mM magnesium acetate, 1% (v/v) 2-mercaptoethanol at pH 4.5). The mixture was then homogenized for ten minutes at 4 °C, strained through two layers of cheesecloth, and then left on ice for one hour. The material was clarified by centrifugation at 20,000 ***g*** for 20 minutes, and the supernatant mixed with 10% (w/v) polyethylene glycol (PEG) 8000 and stirred overnight. Virus was again pelleted from the mixture by centrifugation at 20,000 ***g*** for 20 minutes, and the isolated pellet dissolved over 12 hours in a 1:10 diluted extraction buffer. The solution was then clarified, mixed with 15% PEG 8000, pelleted and resuspended as described above.

Final purification was achieved by mixing the virus solution with $CsCl_2$ to a refractive index of about 1.3806 and centrifuging for 24 hours at 110,000 ***g***. The milky white band of virus was removed by puncturing the side of the centrifuge tube with a syringe. After dialysis for 24 hours against 1:10 diluted extraction buffer at 4 °C, virus was concentrated in Centricon concentrators to about 7 mg/ml.

Crystallization

Rhombohedral BMV crystals were obtained by mixing 10 µl of virus solution with 10 µl of 23% polyethylene glycol 550 mono-methyl ether containing 0.1 M magnesium acetate at pH 5.2. The drops were then equilibrated at 18 °C by vapor diffusion with 1.0 ml reservoirs in Cryschem plates (Hampton Research, Laguna Niguel) sealed with clear plastic tape. Crystals were visible after about seven days and grew to about 1 mm × 1.5 mm in 10-15 days.

Diffraction studies

Rhombohedral BMV crystals were exposed for about 60 seconds to a cryoprotectant mixture consisting of one part precipitant, one part glycerol, and one part PEG 400, and excess solid sucrose. Crystals were then passed repeatedly through perritone oil to remove excess cryoprotectant prior to flash cooling in a liquid nitrogen stream. Crystals diffracted to about 3.4 Å and data were collected at the Advanced Light Source, Beamline 5.0.2.

Images were collected with an oscillation angle of 1.0° and processed using a mosaicity of 0.9. Raw images were reduced using DENZO and SCALEPACK.[33] Separate runs of DENZO were required to process the full dataset and each run of DENZO arbitrarily chose one of the two possible indexing schemes for the *R*3 space group. In SCALEPACK, each set of indexed images from DENZO was then subsequently compared to each other in both orientations and the best set of orientations was used for the final data set. The crystals were of rhombohedral space group *R*3 with unit cell dimensions of $a = b = c = 263.5$ Å, $\alpha = 61.5°$ (equivalent centered hexagonal cell of $a = b = 269.2$ Å, $c = 638.1$ Å, $\alpha = \beta = 90°$, $\gamma = 120°$). A total of 2,463,817 observations were reduced to 203,504 unique reflections with an overall $R_{sym} = 0.170$. The data set was 86.4% complete to 3.4 Å as presented in Table 1.

Table 1. Data processing statistics

Shell lower limit (Å)	Upper limit (Å)	Average *I*	Average error	Stat.	Normal chi*2	Linear *R*-factor	Square *R*-factor	Completion
100.00	9.77	1368.3	198.2	94.6	0.452	0.055	0.067	86.3
9.77	7.75	766.0	110.5	51.9	0.589	0.070	0.079	93.8
7.75	6.77	435.9	66.5	34.7	0.775	0.098	0.102	94.8
6.77	6.16	291.2	49.3	29.7	0.880	0.129	0.128	96.0
6.16	5.71	222.4	42.6	28.5	0.970	0.165	0.150	96.4
5.71	5.38	243.9	46.9	31.6	1.037	0.174	0.162	96.5
5.38	5.11	252.4	49.5	33.8	1.081	0.184	0.174	95.8
5.11	4.89	219.7	47.5	34.4	1.133	0.214	0.200	95.1
4.89	4.70	204.9	47.8	36.0	1.188	0.236	0.211	94.6
4.70	4.54	201.0	49.1	37.8	1.206	0.250	0.218	93.8
4.54	4.39	179.0	83.8	51.0	0.746	0.282	0.239	93.6
4.39	4.27	167.2	82.1	52.4	0.794	0.309	0.250	93.5
4.27	4.16	141.0	75.9	50.8	0.815	0.354	0.287	93.6
4.16	4.05	103.8	65.5	47.9	0.855	0.453	0.341	93.7
4.05	3.96	76.2	59.2	46.6	0.900	0.601	0.450	94.0
3.96	3.88	72.6	59.4	47.8	0.906	0.656	0.462	94.0
3.88	3.80	69.2	60.2	49.6	0.898	0.695	0.475	91.5
3.80	3.73	53.8	58.4	50.5	0.967	0.859	0.551	80.9
3.73	3.66	56.0	62.8	54.8	0.911	0.820	0.598	73.6
3.66	3.60	45.8	66.4	59.9	0.910	0.000	0.631	69.3
All reflections		260.8	68.6	45.6	0.901	0.170	0.124	91.0

Structure solution and refinement

The virus particle is centered at the origin with an icosahedral 3-fold axis coincident with the body diagonal of the rhombohedral *R*3 cell. Thus, the crystallographic asymmetric unit consists of one-third of a particle, or 60 protein subunits, or 20 ABC trimers. Self-rotation function searches produced 5-fold and 3-fold axes that were consistent with icosahedral symmetry; however, a direct rotation search was used to solve the structure. The coordinates for CCMV were obtained from VIPER (http://mmtsb.scripps.edu/viper/) and expanded to an asymmetric unit (20 ABC trimers) unique to a particular icosahedral 3-fold axis. The model was rotated around the origin to bring this 3-fold axis into coincidence with the body diagonal of the *R*3 cell. The model was then rotated incrementally about the body diagonal. At each position, the correlation coefficient and *R*-factor were calculated. The final direct rotation search included expansion/contraction of the model along the vectors defined by the origin and the centers-of-mass of the 20 trimers in the model, followed by 20 group rigid body refinement

Table 2. Refinement results

Resolution	Number reflections		*R*-value	Accum.	Completeness (%)	Accum. (%)
A. R_{free} *(F>4 sigma in bold)*						
7.32 100	1034	**985**	0.252 **0.206**	0.252 **0.206**	4.36 **4.15**	4.36 **4.15**
5.81 7.32	1157	**945**	0.308 **0.242**	0.273 **0.219**	4.87 **3.98**	4.62 **4.07**
5.08 5.81	1120	**830**	0.351 **0.262**	0.292 **0.229**	4.73 **3.50**	4.65 **3.88**
4.61 5.08	1155	**775**	0.406 **0.266**	0.314 **0.236**	4.87 **3.27**	4.71 **3.72**
4.28 4.61	1163	**686**	0.475 **0.274**	0.338 **0.241**	4.91 **2.89**	4.75 **3.56**
4.03 4.28	1103	**358**	0.577 **0.286**	0.362 **0.244**	4.64 **1.51**	4.73 **3.22**
3.83 4.03	1074	**263**	0.764 **0.320**	0.391 **0.247**	4.53 **1.11**	4.70 **2.92**
3.66 3.83	940	**182**	0.707 **0.320**	0.409 **0.249**	3.97 **0.77**	4.61 **2.65**
3.52 3.66	754	**63**	0.869 **0.420**	0.426 **0.250**	3.17 **0.27**	4.45 **2.38**
3.4 3.52	641	**28**	0.821 **0.398**	0.438 **0.251**	2.70 **0.12**	4.27 **2.16**
B. R_{work} *(F>4 sigma in bold)*						
7.32 100	20,495	**19,362**	0.242 **0.195**	0.242 **0.195**	86.35 **81.58**	86.35 **81.58**
5.81 7.32	21,620	**17,568**	0.286 **0.226**	0.258 **0.206**	91.07 **74.00**	88.71 **77.79**
5.08 5.81	21,653	**16,277**	0.331 **0.239**	0.276 **0.214**	91.39 **68.70**	89.60 **74.76**
4.61 5.08	21,319	**14,341**	0.395 **0.252**	0.298 **0.221**	89.82 **60.42**	89.65 **71.17**
4.28 4.61	20,995	**12,626**	0.455 **0.266**	0.320 **0.227**	88.59 **53.28**	89.44 **67.60**
4.03 4.28	21,192	**7351**	0.587 **0.286**	0.347 **0.230**	89.14 **30.92**	89.39 **61.47**
3.83 4.03	21,110	**5270**	0.701 **0.307**	0.374 **0.234**	89.04 **22.23**	89.34 **55.87**
3.66 3.83	17,637	**2897**	0.771 **0.340**	0.395 **0.236**	74.50 **12.24**	87.49 **50.43**
3.52 3.66	14,875	**1195**	0.860 **0.352**	0.413 **0.237**	62.61 **5.03**	84.72 **45.38**
3.4 3.52	12,467	**376**	0.906 **0.414**	0.427 **0.237**	52.56 **1.59**	81.51 **41.00**
C. *All data*						
3.4 100	203,504		0.428		85.78	

Table 3. Final model statistics

A. *Ramachandran statistics*			
Most favored regions (no., %)		311	68.2
Additional allowed regions (no., %)		122	26.8
Generously allowed regions (no., %)		22	4.8
Disallowed regions (no., %)		1	0.2
B. B *factor statistics* (Å^2)			
Molecule	All	Main-chain	Side-chain
A	102.6	91.5	114.9
B	103.9	91.3	118.1
C	101.2	91.5	113.2
Mg	56.7		
PEG	62.3		
C. *RMSD*			
Bonds (Å)	0.008		
Dihedral (deg.)	29.7		
Angles (deg.)	1.49		
Improper (deg.)	0.69		

with each group defined as an ABC trimer. These searches produced a CCMV-based model yielding a correlation coefficient of 0.325 and an *R*-factor of 0.439. From this model, a skew matrix was determined by rotating the initial model onto the correctly oriented model and a unique set of 20 non-crystallographic symmetry operators was determined.

A correctly positioned CCMV ABC trimer was mutated to the BMV sequence and an NCS-averaged SIGMAA-weighted $2F_o - F_c$ map was calculated. This was the starting point for an iterative process of model rebuilding, refinement (using NCS operators) by simulated annealing and/or conjugate gradient minimization, and calculation of new NCS-averaged SIGMAA-weighted $3F_o - 2F_c$, $2F_o - F_c$, $F_o - F_c$ and composite omit maps for subsequent model rebuilding. A bulk solvent correction was continually applied during this iterative procedure. Averaging masks covered the protein and the interior of the particle. All maps and refinements utilized all data with $F > 4\ \sigma_F$; however, the sparseness of the data beyond 4.0 Å makes this nominal 3.4 Å structure in reality closer to a 4.0 Å structure determination.

Besides the capsid proteins, the model contains two Mg ions and a fragment of polyethylene glycol. The Mg ions were built into $2F_o - F_c$ composite omit electron density maps contoured at about 2.5 σ, one on the quasi-3-fold axis and the other on the 5-fold axis. The PEG, which lies along the three-fold axis, was built into a terminally flared, 22 Å long tube of density in a $2F_o - F_c$ composite omit map contoured at 1 σ. In each case, the identities assigned to these non-protein components were based on the crystallization medium (see Crystallization, above) and the local environment.

The refined model yields an *R*-factor of 0.237 (*R*-free of 0.251) with a $4\sigma_F$ cutoff. Details of the refinement statistics are given in Table 2 and those for model geometry in Table 3. All geometrical statistics are good for a 4.0 Å resolution structure.

Procedures and programs

X-PLOR 3.851[34–36] was used for simulated annealing and conjugate gradient minimization, and PROCHECK[37] for evaluating model quality. Initially X-PLOR 3.851 was used to make maps that were then NCS-averaged with RAVE[38] using masks generated with MAMA.[39] During the later steps of refinement however, CNS[40] was used for averaging with automatic protein masks for bulk solvent corrections and a MAMA mask covering all of the protein and interior of the virus for NCS averaging. Manual rebuilding was carried out using the program O.[41] Surface rendering was achieved with the program GRASP.[42] Ribbon models were made using the Molray interface to Persistence of Vision™ Ray Tracer (POV-Ray™) and MOLSCRIPT,[43] with rendering using Raster3d.[44] Mini-maps were made using the Xcontour Program in XtalView.[45]

Coordinates

The coordinates have been deposited in the RCSB Protein Data Bank (accession code: 1JS9).

Acknowledgments

The authors thank Aaron Greenwood for technical assistance. The research was supported by a grant from the NIH and from NASA.

The Advanced Light Source is supported by the Director, Office of Science, Office of Basic Energy Sciences, and Materials Sciences Division, of the US Department of Energy under contract no. DE-AC03-76SF00098 at Lawrence Berkeley National Laboratory.

Coordinates for the published CCMV structure were obtained from the VIPER site (http://mmtsb.scripps.edu/viper/) which is supported by NIH research resource: Multiscale Modeling Tools for Structural Biology (MMTSB), RR12255.

References

1. Van Regenmortel, M. H. V., Fauquet, C. M., Bishop, D. H. L., Carstens, E. B., Estes, M. K., Lemon, S. M. *et al*. (2000). *Virus Taxonomy: Seventh Report of the International Committee on Taxonomy of Viruses*, pp. 923-928, Academic Press, San Diego.
2. Lane, L. C. (1977). Brome mosaic virus. *CMI/AAB Descript. Plant Viruses*, **180**, 1-4.

3. Ahlquist, P., Allison, R., Dejong, W., Janda, M., Kroner, P., Pacha, R. & Traynor, P. (1990). Molecular biology of bromovirus replication and host specificity. In *Viral Genes and Plant Pathogenesis* (Pirone, T. P. & Shaw, J. G., eds), pp. 144-155, Springer-Verlag, New York.
4. Kaper, J. M. (1975). *The Chemical Basis of Virus Structure, Dissociation and Reassembly*, pp. 333-352, North-Holland, Amsterdam.
5. Argos, P. & Johnson, J. E. (1984). Chemical stability in simple spherical plant viruses, in biological macromolecules and assemblies. In *Virus Structures* (Jurnak, F. A. & McPherson, A., eds), pp. 1-32, John Wiley and Sons, New York.
6. Mandahar, C. L. (1989). Multicomponent viruses. In *Structure and Replication* (Mandahar, C. L., ed.), vol. 1, pp. 109-152, CRC Press, Boca Raton.
7. Speir, J. A., Munshi, S., Wang, G., Baker, T. S. & Johnson, J. E. (1995). Structures of the native and swollen forms of cowpea chlorotic mottle virus determined by X-ray crystallography and cryo-electron microscopy. *Structure,* **3**, 63-78.
8. Lucas, R. W., Kuznetsov, Y. G., Larson, S. B. & McPherson, A. (2001). Crystallization of brome mosaic virus (BMV) and $T = 1$ BMV particles following a structural transition. *Virology,* **286**, 290-303.
9. Incardona, N. L. & Kaesberg, P. (1964). A pH-induced structural change in bromegrass mosaic virus. *Biophys. J.* **4**, 11-21.
10. Yamazaki, H. & Kaesberg, P. (1963). Degradation of bromegrass mosaic virus with calcium chloride and the isolation of its protein and nucleic acid. *J. Mol. Biol.* **7**, 760-762.
11. Bancroft, J. B. (1970). The self assembly of spherical plant viruses. *Advan. Virus Res.* **16**, 99-134.
12. Incardona, N. L., McKee, S. & Flanegan, J. B. (1973). Noncovalent interactions in viruses: characterization of their role in the pH and thermally induced conformational changes in bromegrass mosaic virus. *Virology,* **53**, 204-214.
13. Caspar, D. L. D. (1963). Assembly and stability of the tobacco mosaic virus particle. *Advan. Protein Chem.* **18**, 37-118.
14. Pfeiffer, P. & Hirth, L. (1974). Aggregation states of brome mosaic virus protein. *Virology,* **61**, 160-167.
15. Bancroft, J. B., Hills, G. J. & Markham, R. (1967). A study of the self-assembly process in a small spherical virus. Formation of organized structures from protein subunits *in vitro*. *Virology,* **31**, 354-379.
16. Bancroft, J. B., Hiebert, E. & Bracker, C. E. (1969). The effects of various polyanions on shell formation of some spherical viruses. *Virology,* **39**, 924-930.
17. Pfeiffer, P., Herzog, M. & Hirth, L. (1976). RNA viruses: stabilization of brome mosaic virus. *Phil. Trans. Roy. Soc. ser. B,* **276**, 99-107.
18. Krol, M. A., Olson, N. H., Tate, J., Johnson, J. E., Baker, T. S. & Ahlquist, P. (1999). RNA-controlled polymorphism in the *in vivo* assembly of 180-subunit and 120-subunit virions from a single capsid protein. *Proc. Natl Acad. Sci. USA,* **96**, 13650-13655.
19. Bancroft, J. B., Bracker, C. E. & Wagner, G. W. (1969). Structures derived from cowpea chlorotic mottle and brome mosaic virus protein. *Virology,* **38**, 324-335.
20. Johnson, J. E. & Rueckert, R. (1997). Assembly of spherical viruses. In *Structural Biology of Viruses* (Chiu, W., Burnett, R. M. & Garcea, R. L., eds), Oxford University Press, Oxford, UK.
21. Leimkuhler, M., Goldbeck, A., Lechner, M. D. & Witz, J. (2000). Conformational changes preceding decapsidation of bromegrass mosaic virus under hydrostatic pressure: a small-angle neutron scattering study. *J. Mol. Biol.* **296**, 1295-1305.
22. Zhao, X., Fox, J. M., Olson, N. H., Baker, T. S. & Young, M. J. (1995). *In vitro* assembly of cowpea chlorotic mottle virus from coat protein expressed in *Escherichia coli* and *in vitro*-transcribed viral cDNA. *Virology,* **207**, 486-494.
23. Jacrot, B., Chauvin, C. & Witz, J. (1977). Comparative neutron small-angle scattering study of small spherical RNA viruses. *Nature,* **266**, 417-421.
24. Chauvin, C., Pfeiffer, P., Witz, J. & Jacrot, B. (1978). Structural polymorphism of bromegrass mosaic virus: a neutron small angle scattering investigation. *Virology,* **88**, 138-148.
25. Anderegg, J. W., Wright, M. & Kaesberg, P. (1963). An X-ray scattering study of bromegrass mosaic virus. *Biophys. J.* **3**, 175-182.
26. Rao, A. L. N. & Grantham, G. L. (1995). Biological significance of the seven amino-terminal basic residues of brome mosaic virus coat protein. *Virology,* **211**, 42-52.
27. Schmitz, I. & Rao, A. L. N. (1998). Deletions in the conserved amino-terminal basic arm of cucumber mosaic virus coat protein disrupt virion assembly but do not abolish infectivity and cell-to-cell movement. *Virology,* **248**, 323-331.
28. Larson, S. B. & McPherson, A. (2001). Satellite tobacco mosaic virus RNA: structure and implications for assembly. *Curr. Opin. Struct. Biol.* **11**, 59-65.
29. Kaper, J. M. & Geelen, J. L. (1971). Studies on the stabilizing forces of simple RNA viruses. II. Stability, dissociation and reassembly of cucumber mosaic virus. *J. Mol. Biol.* **56**, 277-294.
30. Ban, N., Larson, S. B. & McPherson, A. (1995). Structural comparison of the plant satellite viruses. *Virology,* **214**, 571-583.
31. Adolph, K. W. (1975). The conformation of RNA in cowpea chlorotic mottle virus: dye-binding studies. *Eur. J. Biochem.* **53**, 449-455.
32. Pfeiffer, P. (1980). Changes in the organization of bromegrass mosaic virus in response to cation binding as probed by changes in susceptibility to degradative enzymes. *Virology,* **102**, 54-61.
33. Otwinowski, Z. & Minor, W. (1997). Processing of X-ray diffraction data collected in oscillation mode. In *Methods in Enzyme Macromolecular Crystallography* (Carter, J. W. M. J. & Sweet, R. M., eds), pp. 307-326, Academic Press, San Diego.
34. Brünger, A. T. (1991). Simulated annealing in crystallography. *Annu. Rev. Phys. Chem.* **42**, 197-223.
35. Brünger, A. T. (1992). The free *R* value: a novel statistical quantity for assessing the accuracy of crystal structures. *Nature,* **355**, 427-474.
36. Brünger, A. T., Kuriyan, J. & Karplus, M. (1987). Crystallographic *R* factor refinement by molecular dynamics. *Science,* **235**, 458-460.
37. Laskowski, R. A., MacArthur, M. W., Moss, D. S. & Thornton, J. M. (1993). PROCHECK: a program to check the stereochemical quality of protein structures. *J. Appl. Crystallog.* **26**, 283-291.
38. Jones, T. A. (1992). A, yaap, asap, @#*? A set of averaging programs. In *Molecular Replacement* (Dodson, E. J., Gover, S. & Wolf, W., eds), pp. 91-105, SERC Daresbury Laboratory, Warrington, UK.

39. Kleywegt, G. J. & Jones, T. A. (1993). Masks made easy. *CCP4/ESF-EACBM Newsletter Protein Crystallog.* **28**, 56-59.
40. Brünger, A. T., Adams, P. D., Clore, G. M., DeLano, W. L., Gros, P., Grosse-Kunstleve, R. W. *et al*. (1998). Crystallography & NMR system: a new software suite for macromolecular structure determination. *Acta Crystallog. sect. D*, **54**, 905-921.
41. Jones, T. A. & Kjeldgaard, M. (1994). *O-The Manual, version 5.10*, Uppsala University Press, Uppsala.
42. Nicholls, A., Sharp, K. A. & Honig, B. (1991). Protein folding and association: insights from the interfacial and thermodynamic properties of hydrocarbons. *Proteins: Struct. Funct. Genet.* **11**, 281-296.
43. Kraulis, P. J. (1991). MOLSCRIPT: a program to produce both detailed and schematic plots of protein structures. *J. Appl. Crystallog.* **24**, 946-950.
44. Merritt, E. A. & Bacon, D. J. (1997). Raster3D: photorealistic molecular graphics. *Methods Enzymol.* **277**, 505-524.
45. McRee, D. E. (1999). XtalView/Xfit - a versatile program for manipulating atomic coordinates and electron density. *J. Struct. Biol.* **125**, 156-165.

Edited by I. A. Wilson

(Received 23 August 2001; received in revised form 20 December 2001; accepted 20 December 2001)